3

Carruthers, D. J., 2003, Modeling of secondary petroleum migration using invasion percolation techniques, *in* S. Düppenbecker and R. Marzi, eds., Multidimensional basin modeling, AAPG/Datapages Discovery Series No. 7, p. 21–37.

Modeling of Secondary Petroleum Migration Using Invasion Percolation Techniques

Daniel J. Carruthers

Permedia Research Group Inc., Ottawa, Ontario, Canada

ABSTRACT

At the timescales associated with secondary migration, the balance between the gravity and the capillary forces (i.e., the Bond number) overwhelmingly controls the trajectories and characteristics of hydrocarbon flows. At these low flow rates, viscous forces are negligible and can effectively be ignored. From a practical standpoint, this means that techniques used for modeling petroleum flows at production timescales introduce computational overkill and may in fact be entirely inappropriate for solving the petroleum migration problem.

New invasion-percolation (IP)-based techniques have been developed that take advantage of the special force regime of petroleum migration (IP is based on the premise that flow in porous media can be represented by an invasion through a matrix of pores and throats represented by threshold pressures or probabilities; invasion occurs along the fluid front by accessing the ''pore'' with the smallest threshold pressure). The result of this work is the capability to simulate one-phase, constant-composition petroleum flow in models containing tens of millions of grid cells in a matter of minutes, while honoring the mechanics of migration transport. Because the calculation is so fast, these simulations may be extended beyond the transport problem to include other, more time-intensive calculations with very little loss in overall simulation performance.

INTRODUCTION

This chapter will introduce a set of new techniques for simulating the transport processes controlling secondary petroleum migration. These techniques will be shown to honor the physics of migration while being computationally very efficient. It will be argued that modeling techniques based on reservoir production timescales (e.g., Darcy-based solvers) are not required to solve the transport problem for petroleum migration operating on a geologic timescale because of the differences in the force balances between production and migration flow regimes.

This chapter assumes a distinction between migration transport processes and secondary petroleum migration in general. The first (and the subject of this chapter) deals with the mass transfer of petroleum through the porous carriers and baffles in the subsurface. In contrast, *secondary petroleum migration* is a bucket term used to denote the entire petroleum system as

it affects the transport processes over geologic time. Such system components would include generation, expulsion, carrier and seal geometry dynamics, and compositional alternations. These will not be directly covered in this chapter.

This chapter begins with a background on petroleum transport research with the goal of identifying common insights from the research results. Following this is a brief overview of invasion-percolation (IP) modeling with special emphasis on how it can be used to model petroleum migration flows while honoring the findings of the migration transport research.

Finally, novel IP tools will be introduced and applied to a variety of test cases to demonstrate their flexibility and speed in solving the transport problem. The chapter will then conclude with a discussion of the implications of the work and suggest ways of extending the techniques to assist in modeling secondary petroleum migration in general.

BACKGROUND ON PETROLEUM MIGRATION TRANSPORT PROCESSES

This section presents a brief review of previous published research into secondary petroleum migration, with the aim of elucidating the basic mechanics of fluid flow (specifically the invasion of a nonwetting[1] phase into a water-saturated medium) operating over geologic timescales. It is divided into two main sections. The first reviews past theoretical speculations of the mechanics of secondary petroleum migration, and a brief review of physical models and laboratory-based experiments follows.

Theoretical Considerations

As will be shown, it is commonly accepted that capillary pressures have an overwhelming effect on petroleum flow in carrier beds. Indeed, it is generally accepted that although buoyancy drives the petroleum through the porous media, it is the fabric of the capillary pressures in the porous media that controls trajectories and saturations. The driving buoyancy force originates from the density contrast between the petroleum phase and the surrounding formation waters. Where the buoyancy (or joint buoyancy and viscous) force exceeds the capillary force, the system is said to be out of capillary equilibrium, or gravity destabilized, and flow will occur.

For this destabilization to occur through a given rock volume, a critical column height (pressure head) is required. Berg (1975) described this relationship between capillary pressure and petroleum transport and showed that the critical height is a function of the fluid-fluid interfacial tension, the pore throat radii, and the phase densities (equation [1]).

$$z_c = \frac{2_\gamma\left(\frac{1}{r_t} - \frac{1}{r_p}\right)}{g(\rho_w - \rho_o)} \qquad (1)$$

where γ is the fluid-fluid interfacial tension, r_t is the pore throat radius in the barrier/caprock, r_p is the pore throat radius in the reservoir rock, g is acceleration caused by gravity, ρ_w is the water density, ρ_o is the oil density, and z_c is critical column height.

Equation (1). Critical height for petroleum migration.

In Berg's view, petroleum migrates to a pore throat, where it remains trapped (and discontinuous from adjacent petroleum-saturated pores) as long as its buoyancy pressure is lower than the capillary pressure of the pore throat. Once additional petroleum volume becomes available, the length of the petroleum ganglia will grow through coalescence to the point where the critical height is reached, and flow will occur (see Figure 1).

If equation (1) is solved for a variety of plausible pore throat radii, then it can be shown that "the critical height is many times larger than the dimensions of pores, or, in other words, the vertical length of

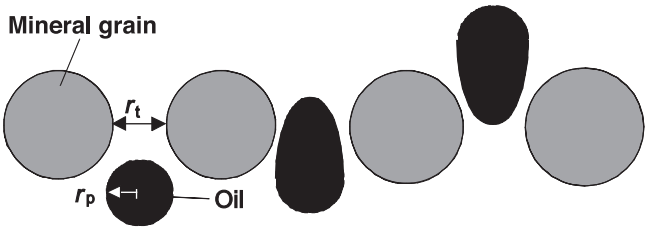

Figure 1. Migration mechanism, according to Berg (1975).

[1]The concept of a wetting phase can be explained through the process of surface energy or surface tension, where there exists an imbalance in the molecular forces in a fluid-fluid interface. Water has a very high value of surface tension, because it has a high degree of hydrogen bonding. Organic molecules have a lower surface energy than water. The interactions between the high surface tension of water and surface chemistry conditions result in most mineral grains having water as the preferred wetting phase. When given the choice between being coated with petroleum and water, most minerals prefer water, with the implication that migration is primarily a drainage process (wetting phase decreasing).

the oil in continuous phase is such that petroleum migration probably takes place in the form of 'stringers' rather than 'globules.' "(Berg, 1975)

Petroleum, therefore, migrates as a discrete, separate phase, whose trajectory and accumulation history is predictable provided that sufficient information is available concerning the capillary entry pressure distribution of the carrier system.

Berg (1975) cites an example and consequence of using equation (1) to estimate hydrocarbon column heights. Because of a greater density differential, a capillary baffle is more likely to breach under the presence of a gas phase than an oil phase:

> To migrate upward through a fine-grained sandstone with mean grain size of 0.2 mm, a stringer of low gravity oil ($\Delta\rho$ = 0.1 [g/cc]) must be about 300 cm in vertical length. This oil would have sufficient buoyancy to overcome the capillary pressure in pore throats of the rock. On the other hand, a stringer of gas ($\Delta\rho$ = 1.0 [g/cc]) need only be about 30 cm in vertical length to overcome the capillary pressure in the pore throats because of its greater buoyancy. (Berg, 1975)

As will be shown, this capillary-dominated, pulse-feeding mechanism accords with laboratory-based experiments and will play a key role in defining the algorithm used to simulate migration transport.

Schowalter (1979), whose paper focused on the mechanics of secondary hydrocarbon migration and entrapment, supported Berg's ideas. As with Berg (1975), Schowalter (1979) takes the position that oil migrates as a single, continuous phase, not only principally caused by the effects of buoyancy but also caused by the presence of hydrodynamic gradients. Oil migrates until it reaches a point of gravity equilibrium (where the driving forces of buoyancy are equilibrated with the opposing, dissipative capillary forces).

The factors that determine the magnitude of this dissipative force are (1) the radius of the pore throats of the rock, (2) the hydrocarbon-water interfacial tension, and (3) wettability. These factors in combination are generally called "capillary pressure."

Again, capillary pressure is recognized as being the dominant control on migration transport. Schowalter (1979) goes on to note that it is specifically the capillary displacement (threshold) pressure that is the controlling parameter, because it defines "the pressure required to form a continuous filament of nonwetting fluid through the largest connected pore throats of the rock." From the transport perspective, this is extremely significant, because it defines at what point the oil phase relative permeability is nonzero (Figure 2) and hence, at what point the mobilization of the petroleum across a given volume will occur.

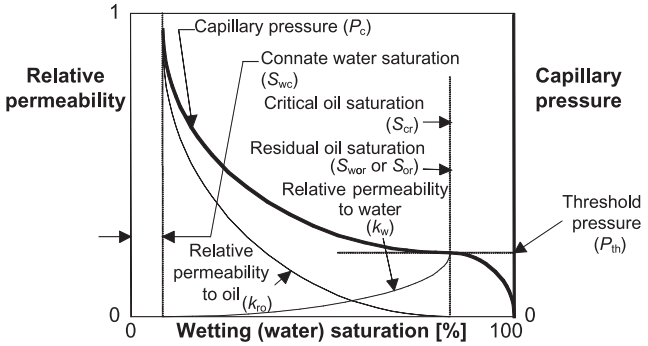

Figure 2. Saturation functions and their relationship to displacement (threshold) pressure.

Specifically, this threshold pressure is the pressure "which will determine the minimum buoyant pressure required for secondary petroleum migration." Schowalter (1979) suggests that the threshold pressure can be inferred from standard mercury intrusion experiments and corresponds with the "capillary plateau" or inflection point of the capillary pressure curve (Figure 2).

England et al. (1987) support the notion that petroleum will flow through a given rock volume at a critical saturation, specifically, the "fractional oil saturation at which the sample of rock first contains interconnecting pathways."

> Petroleum will only migrate as far (and as fast) as the volume of petroleum expelled from the source rock can spread out whilst remaining fully interconnected. After migration, a volume of petroleum will be left in the sequence. This residual volume will be similar to that necessary to connect both sides of the sequence with flowing petroleum. There are two supporting arguments for these assumptions: the dominance of capillary forces implied by low capillary numbers and the field evidence of petroleum-stained rock. (England et al., 1987)

England et al. (1987) also suggest that viscous forces will be insignificant for petroleum migration. This extremely important insight is based on the authors' calculations of the source rock expulsion rates, which, as the authors suggest, is the dominant

control on secondary petroleum migration velocities. Values between 8×10^{-10} and 4×10^{-14} $m^3/m^2/s$ are suggested as being realistic. From these rates, one can calculate the capillary number (ratio of viscous to capillary forces) using equation (2):

$$C_a = \frac{\mu \cdot q}{\gamma} \qquad (2)$$

where C_a is the capillary number, μ is the dynamic viscosity, q is the Darcy flux per unit cross-sectional area, and γ is the interfacial tension.

Equation (2). Capillary number.

England et al. (1987) state that ''experiments with oil-water mixtures in rocks have shown that at capillary numbers greater than 10^{-4}, viscous forces become important. However, at geological flow rates, the capillary number is never greater than 10^{-10}. Capillary forces, therefore, dominate at all times.''

If this is true, then the only parameters required for solving the transport problem are those that affect the capillary or buoyancy forces (see Figure 3; Carruthers and Ringrose, 1998). Restated, factors such as viscosity and permeability are irrelevant.[2] In fact, according to England et al. (1987), the capillary number for migration is six orders of magnitude away from the point at which viscous forces are significant.

Summary of Theoretical Work

These reviewed works offer common insights into the mechanics of petroleum transport. Specifically,

1) oil is fed into carrier beds from source horizons at capillary-dominated, geologic flow rates;
2) migration occurs as a series of pulses, with discontinuities occurring in the petroleum phase;
3) capillary and gravity (buoyancy) forces will always dominate over viscous forces;
4) each discrete volume of rock will have a threshold pressure at which the invading petroleum phase will form a cluster of saturated pores across the volume;
5) the saturation coinciding with this threshold pressure is the critical saturation for migration through the discrete rock volume.

[2]Although permeability in itself is not relevant, capillary threshold pressure is, and by definition, for a rock volume to have a threshold pressure, it must be permeable. However, in solving the transport problem, permeability and relative permeability are not variables that are required.

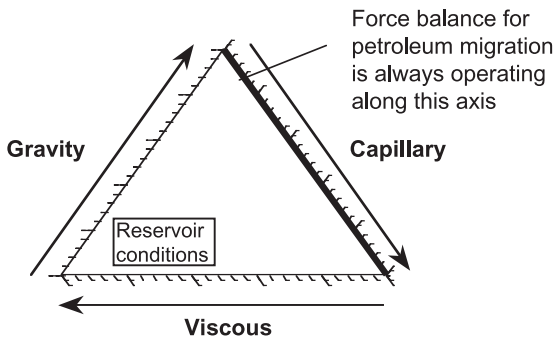

Figure 3. Forces affecting petroleum migration. Viscous forces are insignificant, suggesting that tools for solving the transport problem associated with reservoir and production timescales are inappropriate for solving migration transport.

The next section reviews experimental work and will show that these postulations are indeed valid.

Physical Models and Laboratory-based Experiments

Dembicki and Anderson (1989) constructed simple petroleum migration models using cylindrical glass columns packed with quartz grains. These columns were filled with a water-sediment slurry, and a small volume of oil was loaded onto the top of the column. The column was then inverted, and the oil's vertical migration was observed. The procedure was then repeated for nonvertical columns.

They observed the following.

1) In all their configurations, the oil always moved through the sediment along focused and restricted pathways.
2) Residual oil was left behind, along the migration pathway, at a volume equal to the spanning cluster (the spanning cluster is defined as the set of connected, petroleum-filled pores that spans two points in space, e.g., between the source area and the reservoir).
3) The migration rates observed were in the order of tens of centimeters per hour, suggesting that the carrier can accommodate flow volumes much greater than required to fill reservoirs within reasonable timescales and certainly orders of magnitude greater than expulsion rates from source rocks.

Although their models were simplistic, they are useful in suggesting that petroleum migration may be a very efficient process (at least through low-threshold-pressure carriers) caused by the low volume of the migration conduits. They also observed

that the oil volume and saturation that were left behind (the residual oil) were essentially the same as the volume of the spanning cluster (i.e., the critical oil saturation). This suggests a direct relationship between the residual volume and the critical saturations and also supports the postulations of Berg (1975), Schowalter (1979), and England et al. (1987).

More recently, Catalan et al. (1992) performed a series of experiments designed to simulate secondary petroleum migration through glass bead packs and sand columns. They used oils of various densities, which also covered a range of interfacial tensions. In addition, they looked at the effect of carrier dip angle by modifying the column orientation.

The configuration of their bead or sand columns was nearly identical to Dembicki and Anderson's (1989), and many of the observations made by Dembicki and Anderson (1989) were reproduced. Specifically, they noted that the oil migrated along restricted, highly focused pathways (the scale of the oil stringers was in the order of 1 cm in width) and that the oil was left behind in the migration pathway in about the same volume as the amount needed to span the inlet and the outlet (i.e., the volume of the spanning cluster).

Catalan's group also observed that the migration rate was constant for a given set of conditions and that this constant rate was highly affected by the oil volume used as a source. In fact, the migration velocity was directly proportional to the feeding rates and volumes: the higher the feeding volume, the higher the velocity. This implies that the migration rate may be a function of the feeding mechanism, independent of the carrier system properties. In other words, over the timescales associated with petroleum migration, the invading fluids quickly equilibrate to the force conditions and no time-controlling properties, such as permeability and viscosity, will control the transport processes to the same degree as the force balances.

In explaining their observation of a constant flow rate, Catalan et al. (1992) group made an interesting observation: ''the oil permeability is dependent on the type of displacement process (migration versus gravity-stable displacement).'' They noted that the oil saturations are fairly constant throughout the oil column, and because the relative permeability of the oil front is a function of the oil saturation, one can expect the relative permeability to be constant throughout the oil cluster. Most relative permeability curves measured in the laboratory or published in the literature are based on gravity-stable conditions. In other words, the buoyancy forces are negligible (caused by the length scale of the samples), with the oil and water tending to be displaced throughout the sample rather than confined to restricted pathways as is the case in gravity-destabilized displacement. ''Consequently, the relative permeability to oil would be larger for petroleum migration than for a gravity-stable displacement for the same oil saturation.'' (Catalan et al., 1992).

This implies that any given volume of carrier material may have a single relative permeability value to oil, because the oil saturation through that volume will be constant (at the so-called critical saturation) once the volume is spanned by the oil phase.

Catalan et al. (1992) also noted that the oil moved through the system with ''disconnections occurring near the migration front [that] reduced the height of the rising filaments below the minimum height for migration and cause the migration front to stop until enough oil was supplied from the lower parts of the column to reconnect the temporarily stranded filaments.'' As the oil moves through the system, the saturation is essentially constant, with the expansion occurring at the displacement front. Once a volume is spanned, the oil saturation in that volume is constant.

These observations are critical in that they suggest that the migration rate is a function of the feeding rate and that discontinuities in the invading phase will occur, having an obvious impact on localized pressure heads in the petroleum phase. This is experimental evidence of the migration mechanisms proposed by Berg (1975), Schowalter (1979), and England et al. (1987).

Thomas and Clouse (1995) further supported the idea that migration velocities are a function of the feeding mechanisms. Thomas and Clouse's (1995) physical model was designed to simulate gravity and capillary-controlled oil flow through a pristine, water-saturated carrier bed. The purpose of their model was to ''provide both visualization of the flow patterns and estimates of hydrocarbon transport rates and efficiencies.''

Thomas and Clouse (1995) noted that the rate-limiting step in charging a trap is not secondary migration (i.e., permeability or viscous effects) but rather the expulsion rate from source rocks. If the source rock controls the migration velocity, then this implies (as already noted) that the carrier system equilibrates instantaneously to the fluid pressure conditions (i.e., operates under a state of capillary equilibrium). Certainly, if they observed equilibrium in their models

over a short (human) timescale, then one can expect equilibrium when dealing with the geologic timescales associated with the secondary petroleum migration system in general.

This also suggests that migration velocities can be estimated by calculating the volumetric flux rates from a source horizon and that these flux rates should be of the same order of magnitude that one can expect to occur in a carrier system.

Frette et al. (1992) conducted experiments in which they looked at ''the slow upward migration, caused by buoyancy, of a nonwetting fluid through a saturated, three-dimensional porous medium.'' The authors used random packings of cylindrical grains (2 mm in diameter, 2 mm in length) of transparent Plexiglas.

Frette's group found that the saturation profile and the trajectories of the invading phase were a function of the Bond number (equation [3]). When the Bond number increases, the invading cluster becomes more focused; when it decreases, the invading cluster tends to spread laterally and greater column heights are required to breach any baffles.

$$B_o = \frac{\Delta\rho \cdot g \cdot x^2}{\gamma} \qquad (3)$$

where B_o is the Bond number, $\Delta\rho$ is the density difference between the two fluids, g is the acceleration caused by gravity, x is the length scale, and γ is the fluid-fluid interfacial tension.

Equation (3). Bond number, defined as the ratio of gravity (buoyancy) and capillary forces.

In addition, Frette et al. (1992) noted a steplike motion of the displacement structure (similar to that observed by Catalan et al., 1992, and proposed by Berg, 1975). Frette et al. (1992) noted:

> One manifestation of the complex dynamics of this growth process was the structure of h(M) and the step-like motion of the displacement structure tip. In connection with these bursts the structure sometimes ''snapped off'' and disconnected parts could move independently some distance upward. Further snapoffs diminished the length of the moving, disconnected parts until they were stuck in the matrix. The uppermost point would then move only after reconnection from the main structure (fluid was being slowly injected from the bottom point).

This phenomenon is shown in Figure 4.

The observed cycle of migration-snapoff-reconnection-migration of the invading fluid has implications for how the pressure head of the petroleum should be calculated in any simulation tool. The column height that actually drives migration at any instant is not the distance from the source to the tip of the invading cluster but rather from the base of the ''snapped-off'' ganglion to the uppermost tip of the invading cluster. In this way, the gravity component will not increase linearly with the total height of the invading cluster—it will instead depend on the dynamics of the invasion process, being a function of the characteristics of the petroleum cluster through time. Any transport simulator that assumes ubiquitous connectivity in the petroleum phase will not be representing the fluid conditions of migration transport.

Evidence for the snapoff phenomenon was reported from field experience in 1997, in which Rasmussen (1997) used transmitted-light-scanning electron microscopy to examine minute rims of bitumen that were found surrounding detrital radioactive grains taken from Australian Permian-Triassic sandstones. According to Rasmussen (1997), the appearance of bitumen on the mineral surface is indicative of a former presence of liquid hydrocarbons.

When these bitumen coatings were subjected to blue-violet epifluorescent illumination, they exhibited complex concentric and contorted banding that the author

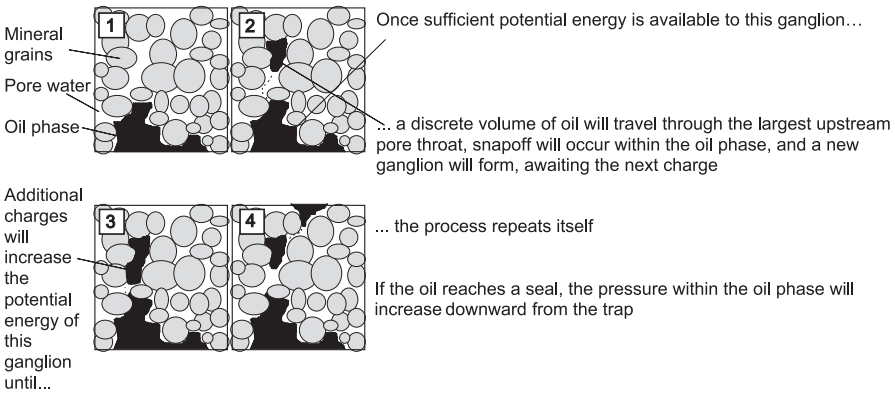

Figure 4. Mechanism of fluid migration as observed by Frette et al. (1992).

attributes to multiple oil charges and successive influxes of a liquid hydrocarbon phase. The process is summarized in Figure 5.

Based on these observations, it would appear that the petroleum does indeed migrate as a series of pulses. Once sufficient buoyancy pressure is available to overcome the capillary entry pressure of the largest upstream pore throat, the oil will migrate, snapping off at a deeper level, creating a series of isolated stringers. If we consider a two-stringer scenario, then one would expect the concentric banding observed by Rasmussen (1997) to occur in the area between the lower end of the higher stringer and the upper end of the lower stringer. The pore space in this zone has seen the passing oil phase, and although the phase is no longer present, it has had the opportunity to coat the mineral surfaces.

In addition to what the authors already mentioned, other authors who have conducted other investigations into capillary displacement processes have observed this notion of pulse-based migration (e.g., Chatzis and Dullien, 1983). The mechanism is commonly referred to as the ''Haines jump'' after Haines (1930), who first observed the phenomenon.

Summary of Migration Transport Mechanisms

Each of the physical models and theoretical works reviewed in the last section has highlighted some fundamental mechanisms of how an oil phase behaves as it invades a porous medium at capillary dominated flow rates.

1) Petroleum migrates via a series of pulses defined by a series of charge-accumulate-breach sequences occurring at multiple length scales.
2) The rate of advancement of the invading petroleum phase is a function of the source injection (feeding) rate.
3) The petroleum phase follows highly focused flow pathways defined by the balance between driving (buoyancy) and dissipative (capillary) forces (i.e., the so-called Bond number).
4) For flow to occur across a given volume, the petroleum phase needs to form a spanning cluster of saturated pores across the sample volume. Flow is concentrated in this spanning cluster.
5) A critical (threshold) pressure is required for a spanning cluster to form. Threshold pressures will control column heights and act as switches as to whether flow can occur or not.

The next section looks at IP, which is a process that has long been used (at least in the physics literature) to simulate the invasion of a nonwetting phase into a wetting-phase-saturated porous medium. One assumption of IP is that the invasion occurs in a state of capillary equilibrium and that viscous forces are negligible. Based on the work presented thus far, these are precisely the conditions operating for petroleum migration flows.

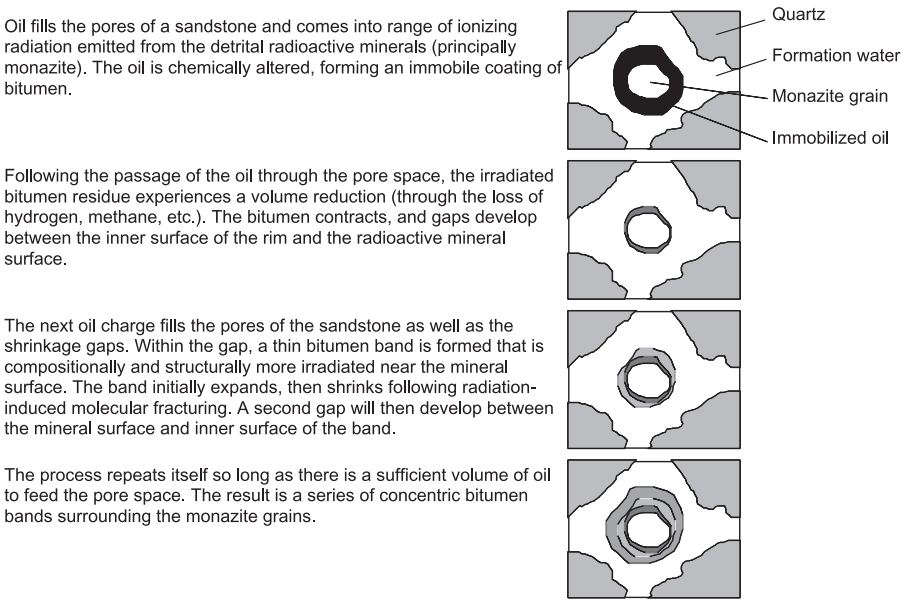

Figure 5. Evidence for pulse feeding and snapoff, adapted from Rasmussen (1997).

BACKGROUND ON INVASION PERCOLATION

Percolation theory is concerned with the state of networks or bonds in heterogeneous systems. In its simplest form, percolation theory can interpret the behavior of the system shown in Figure 6. Consider each gridline in the example as representing a pipe having its own on-off valve. The question may be asked, ''How many of the pipes (bonds) in the lattice must be turned on before a cluster of activated bonds is formed which spans the lattice, allowing fluid to flow from one boundary to its opposing boundary?'' Percolation theory tells us that for a 2-D lattice

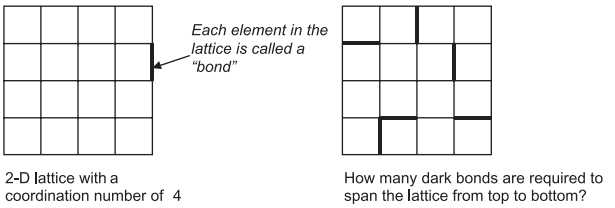

Figure 6. Percolation in its most basic form.

with a coordination number[3] of 4, 50% of the bonds must be ''turned on'' before a spanning cluster is formed between adjacent sides of the model. At this point, the model is said to ''percolate.'' Percolation theory also tells us that for 3-D systems (coordination number of 6), the number of bonds necessary for percolation to occur drops to 26%, due largely to the increase in the coordination number.

Early research (e.g., Broadbent and Hammersley, 1957) was concerned with quantifying the behavior of static networks and focused more on describing the connectivity issues of the lattice itself (similar to the previous example) than on coupling the lattice models with a fluid displacement or transport process. For example, the bonds in Figure 6 would be turned on at random rather than making any attempt at simulating a fluid invasion process. Statistics such as how many activated bonds are required to percolate for various lattice configurations would be collected.

It was not until the late 1970s and early 1980s that several authors addressed the problem of displacement of one fluid by another in the context of percolation theory. Chandler et al. (1982) presented one such paper in which they considered the capillary displacement of immiscible fluids using a percolation process. Chandler et al. (1982) used a lattice to represent a network of capillary tubes that were taken to be analogous to pore throats in a porous medium. The bonds in their model were assigned a radius taken from a random distribution (uniform), and this number was in turn used to calculate the capillary pressure difference that would exist at the pore throat interface according to equation (4).

$$P_c = \frac{\gamma}{r} \tag{4}$$

where P_c is the capillary pressure, γ is the interfacial tension, and r is the pore throat radius.

Equation (4). The capillary pressure difference between fluids is proportional to the interfacial tension between the fluids and the pore throat radius.

A numeric fluid was injected at one of the model's interfaces, and each bond connected to that interface was then invaded. Chander et al. (1982) then performed a series of iterations in which, at each time step, the bond having the lowest capillary threshold pressure and that connected to an invaded bond is itself invaded. This process continues, until the percolation threshold is reached (i.e., a spanning cluster is formed). At this point, the critical saturation may be determined along with the capillary threshold pressure of the spanned volume. (Typical output for such a model is shown in Figure 7.)

In 1983, Wilkinson and Willemsen coined the phrase *invasion percolation*. This type of percolation modeling ''explicitly takes into account the transport process taking place,'' which in their case was of a wetting, invader fluid (water) displacing a nonwetting, defender fluid (oil). The term *invasion percolation* is applied to percolation models in which, at each time step, the displacing fluid configuration grows along the front by occupying the accessible site with the smallest, randomly distributed, capillary threshold pressure. In these models, all growth occurs via a single cluster (as opposed to the randomly populated percolation models, such as the one in Figure 6). As with the Chandler et al. (1982) model, the IP models assume that the viscous forces are insignificant when compared with the capillary

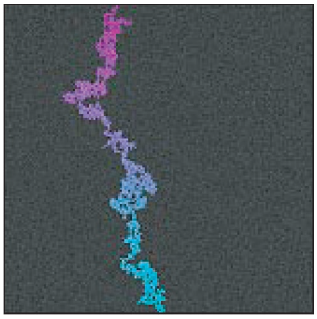

Figure 7. Typical IP model profile.

[3]A coordination number refers to the number of neighboring cells that exist in the lattice. If, for example, the grid cell marked with the × in the first picture below was connected with all the shaded neighbors, its coordination number would be 4. If it was connected to its neighbors as shown in the second picture, its coordination number would be 8.

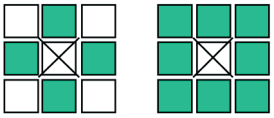

forces because of an assumed infinitesimal flow rate (an ideal assumption for migration modeling).

Wilkinson (1984) extended his work on IP to include the effects of buoyancy (which is of obvious relevance for secondary petroleum migration modeling). In this paper, he considered again the effects of water invading an oil-saturated network and looked at how the fluid interface moves through the network under the constraints of buoyancy. His models considered only the hydrostatic case in which, at any instant, the system is assumed to be in a state of capillary equilibrium.

Invasion percolation is a dynamic process based on stochastically generated flow fields. It is therefore difficult to interpret the system behavior, except in highly idealized systems. Furuberg et al. (1988) discussed this dynamism. They noted that IP has a well-defined sequence of invaded sites; that is, we know the sequence in which the bonds are charged with oil (which has beneficial implications if we want to couple these models with chemical tracking). They also noted that the IP process generates self-similar fractal structures and that the number of sites that contain oil scales with the size of the lattice (this has implications for upscaling critical saturations and threshold pressures).

Meakin et al. (1992) conducted a series of computer simulations to investigate IP with a gravity-destabilized gradient (recall that migration operates under these conditions). In their models, each bond was assigned a random threshold of the form $t_i = X_i + gh_i$, where X_i is a random number distributed over the range [0,1] and h_i is the height (y-coordinate) of the bond. The gravity component (gh_i) is calculated by assuming that the invading fluid (oil) is in constant pressure communication with the source inlet.

They noted that as the gradient (g) was increased, the displacement pattern became more focused (i.e., fewer bonds were invaded before a spanning cluster was formed, consistent with the findings of Catalan et al., 1992). Specifically, in two dimensions, the cluster correlation length ξ_w (where ξ_w is defined as the width of the displacement pattern at a fixed height) has a power law relationship with the gradient (g) (see Figure 8). Extending this observation to ''real'' systems, one would therefore expect that the oil-rock contact volumes would decrease for increasing phase density differences. All things being equal, gas will ''see'' less rock than oil.

Meakin et al. (1992) applied this technique to 3-D systems as well as to systems having nonuniform threshold distributions (e.g., Gaussian and exponential). They found that the mass density (volume per unit length, equation [5]) of the invading cluster had an algebraic dependence on the gradient in both two and three dimensions. They also noted that although the amplitude of this relationship changes for different distributions, the exponent γ does not change. The exponent had a value of 0.473 in two dimensions and 0.690 in three.

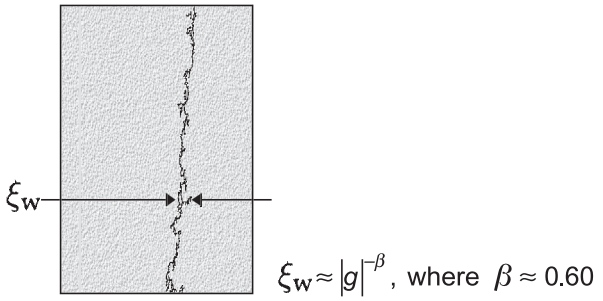

Figure 8. Relationship between gradient and correlation length.

$$M \approx |g|^{-\gamma}. \tag{5}$$

Equation (5). Linear mass density (M) as a function of field strength (g).

Because the gradient term (g) is a measure of the gravity component, there is a direct relationship between equation (5) and the Bond number (recall that the Bond number is defined as the ratio between the buoyancy and capillary forces).

Meakin et al. (1994) extended their work on gradient-driven migration to hydrodynamic gradients. They argue that:

> In the absence of buoyancy effects the hydraulic potential gradient will play the same role as $\Delta\rho g$ in the buoyancy case. [. . .] In general, buoyancy and hydrodynamic effects will act simultaneously so that the migration can be described in terms of the potential (equation [6]). In the buoyancy-destabilized case, the direction of migration will depend on the relative magnitudes of the two components of Φ.

$$\Phi = \Delta\rho g z + \Phi_h. \tag{6}$$

Equation (6). The total migration potential (Φ) is related to the buoyancy force and the static hydraulic potential (Φ_h).

This may provide a way of modeling secondary petroleum migration transport without conducting

an implicit two-phase flow simulation. The capillary pressure field could be modified in advance of the oil invasion by an amount proportional to the hydrodynamic pressure gradient. The oil would then invade through this modified capillary pressure network according to the rules of IP.

Returning to defining the characteristics of the spanning cluster, Hirsch and Thompson (1995) published a paper on the minimum saturations required for migration to occur under gravity-destabilized conditions. In particular, they sought to uncover the relationship between carrier volume and the spanning cluster volume. They note that:

> When the invading fluid spans the network, the invaded fluid structure is a percolation cluster of fractal dimension 2.5. The volume of the percolation cluster thus scales as $V \propto L^{2.5}$, and the total volume scales with $V \propto L^3$, where L is the linear expanse of the cluster. Thus, the saturation varies with the size dimension as:
>
> $$S \propto \frac{L^{2.5}}{L^3}$$
>
> This result suggests that saturation in secondary migration could be very small on the basin scale.

Hirsch and Thompson (1995) also found that the model aspect ratio plays a large factor in determining the critical saturation at breakthrough. They noted that independent of the pore-size distribution, the critical fraction of filled pores at breakthrough decreases with the square root of sample size for 1:1 aspect ratio samples, if the effects of buoyancy are neglected. In addition, ''large aspect ratio (height/diameter) samples have greater saturations than low aspect ratio samples.'' This conclusion has implications for defining representative elementary volumes and for the interpretation of core plug data where boundary conditions will most certainly have affected the results.

Summary of Invasion Percolation Modeling

Invasion percolation may provide an ideal solution for modeling secondary petroleum migration. It uses as its key parameters the capillary thresholds of the medium, as well as considering the phase densities of the invading and defending fluids. These variables have been shown in many ways (in previous sections) to be the dominant controls on secondary petroleum migration, because it appears that only those variables that affect the Bond number are critical for solving the transport problem.

However, two significant limitations of traditional IP algorithms render their direct application to migration transport modeling inconsistent with the mechanisms reviewed earlier.

1) Invasion percolation models assume that the invading phase is ubiquitously connected and therefore in constant pressure communication. As we have seen, oil migrates in discrete, disconnected ganglia. Only where accumulations (at any length scale) begin to form can we assume pressure communication within the petroleum phase. A consequence of IP models not addressing this mechanism is one of scaling. Because IP assumes that the pressure heads are calculated from the base of the invading phase to its uppermost extent, traditional IP models are only applicable to small (submeter) systems (they would certainly not be applicable to the case where there exists a vertical differential of a few kilometers between basin kitchen areas and updip reservoirs).
2) Invasion percolation models assume that the invading phase originates from a single point source. The invading cluster expands from a single point and always into a single point. For a ''real'' petroleum system, where petroleum is being sourced from many concurrent source points and areas, this is a severe limitation.

The next section will demonstrate how we have addressed these limitations while honoring all the mechanisms of petroleum migration transport.

ADAPTING INVASION PERCOLATION TO TRANSPORT MODELING OF PETROLEUM MIGRATION

Significant modifications to the traditional IP algorithm are required if it is to be used for migration transport modeling. The classical algorithm for IP is as follows.

1) Start with an invasion point.
2) Search around this invaded site for the site with the lowest threshold pressure. Invade this new site.
3) Search around the invaded cluster for the site with the lowest threshold pressure and invade it.
4) Repeat step 3 until an appropriate stopping point is reached.

This algorithm ignores gravity; therefore, other authors (e.g., Meakin et al., 1992) modified the capillary

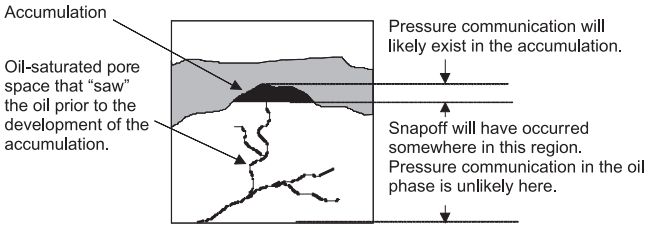

Figure 9. Pressure communication in the petroleum phase can only be assumed within an accumulated state (i.e., the petroleum saturation is greater than the critical saturation).

threshold pressures in the lattice to reflect the vertical pressure gradient imposed by gravity-destabilized conditions. However, it is clear that for large, vertical-scale models, these new, effective threshold pressures can quickly be reduced to zero.

In both cases, the snapoff is ignored, which is the main cause of IP's inability to scale to larger scenarios. As has been discussed, snapoff definitely occurs in the petroleum phase as it migrates, as supported by theoretical work and experimental evidence. This snapoff is associated with saturations near the critical saturation; therefore, continuity in the petroleum phase (and therefore, pressure communication) can only be assumed where saturations are greater than the critical saturation (i.e., in an accumulation, of whatever length scale). Somewhere along the migration pathway, snapoff will have occurred that will break the communication. Where exactly this snapoff has occurred is unimportant. It is sufficient to know that where the oil saturation has increased beyond the critical saturation (e.g., in the development of an accumulation), pressure communication in the oil phase is likely to exist (see Figure 9). Areas outside of the accumulations will likely be riddled with snapoffs in the invading (oil) phase.

Once the classic IP algorithm (without vertical gradients) is modified to reflect these new and appropriate pressure communication assumptions, it is found that models can be created that can perform and simulate core-scale invasions, all the way to basin-scale migration cases. In addition, allowing concurrent development and coalescing of invasion clusters can easily eliminate the single-point feeding limitation. (For a detailed description of this new algorithm, see Carruthers, 1998).

EXAMPLES OF THE NEW TRANSPORT MODEL

This next section provides examples of the new transport model being applied to simple cases for validation purposes, as well as to geologically realistic scenarios ranging from the core to basin scale.

Simple Test Case

Consider the model shown in Figure 10. The model consists of low-, medium-, and high-threshold-pressure flow units (white, gray, and black, respectively) and contains 40,000 grid cells (lattice size of 200 × 200). If we set the low-threshold-pressure units to 1 kPa, the medium-threshold-pressure units to 10 kPa, and the high-threshold-pressure units to 100 kPa, then it is easy to estimate the expected column height beneath each baffle using equation (7) or the graph shown in Figure 11.

$$h = \frac{P_{\text{th}}}{\Delta\rho \cdot g} \tag{7}$$

where h is the column height (m), P_{th} is the capillary threshold pressure of the baffle (Pa), $\Delta\rho$ is the density contrast between the petroleum and water phases (kg/m^3), and g is the acceleration caused by gravity (m/s^2).

Equation (7). Column height supportable by a baffle with a given capillary threshold pressure.

Figure 12 shows a sample simulation created by setting the density contrast to 300 kg/m^3 and using grid cell sizes of differing vertical dimensions. The petroleum is introduced into the system via a single point, located beneath the first baffle, near the base of the model. The true vertical scale of the column heights should remain constant, as the model adjusts to the balance of force scalings for the different Bond numbers.

Indeed, this is precisely what happens, suggesting that the model can be applied to migration problems of varying length scales. In this test case, the threshold pressure of the lower baffle is set to 100 kPa, which would support a 34-m column height of

Figure 10. Test model configuration.

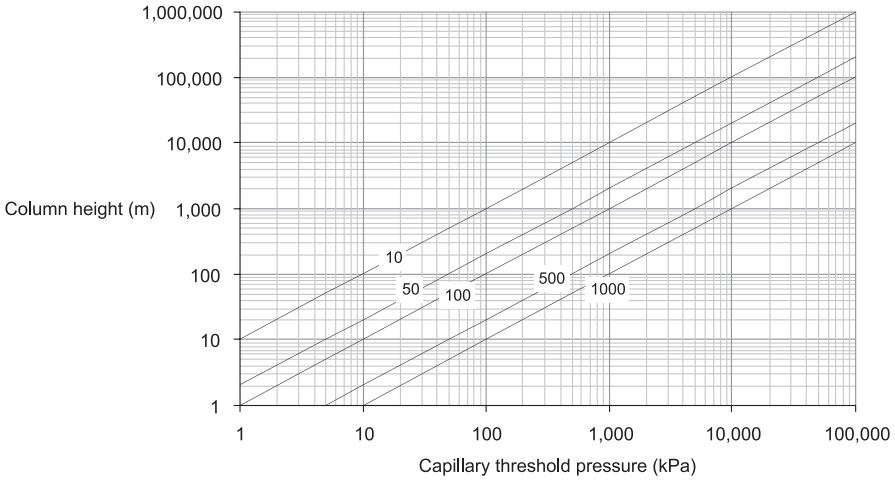

Figure 11. Column height as a function of capillary threshold pressure and density contrast. Density contrast (the difference between the densities of invading and defending phase) is expressed in kilograms per cubic meter.

a petroleum-water system having a density contrast of 300 kg/m^3. In the case of Figure 12a, where the vertical grid cell dimension is set to 1 m, this would equate to 34 grid cells saturated with petroleum before the baffle is breached. This is precisely the outcome of the simulation. When the vertical grid cell size is increased to 2 m, the number of grid cells is halved (17 grid cells); when set to 10 m, the number decreases by a factor of 10, precisely the scaling relationship one would expect (and hope for).

The colors in Figure 12 reflect the accumulation states of the petroleum. Where the invaded sites are represented in light green, the petroleum is assumed to be in an accumulated state (saturation greater than the critical saturation, likely near the connate water saturation), and upwardly directed pressure heads are calculated from this zone. Where the invaded sites are shown in dark green, saturations are equal to the critical saturation, and the petroleum is assumed to be disconnected.

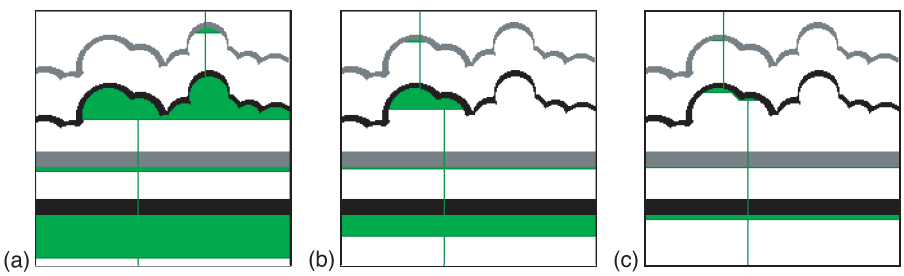

Figure 12. Saturation profiles for the test model when grid cell sizes are set to (a) 1, (b) 2, and (c) 10 m, in all directions. Light green shows oil in an accumulated state; dark green represents oil at the critical saturation. Density contrast is a constant 300 kg/m^3.

The same effects of scaling can be achieved by changing the density contrasts (as predicted by the Bond number definition in equation [3]). This is shown in Figure 13, where the densities have been changed to be roughly analogous to the contrasts one would expect for an oil-water and a gas-water system. In this case, the ''gas'' system breaches the baffles that have lower column heights than in the ''oil'' system because of the higher buoyancy of the lighter petroleum phase, precisely what is estimated from theoretical and experimental evidence.

Moreover, these last two examples highlight the Bond number dependency of the saturation profiles and the petroleum system's selection of migration trajectories. An interesting product of this dependency is that it is very likely that gas and oil would follow different migration pathways given the differences in their Bond numbers, even under hydrostatic conditions.

Having shown the proper force balance scalings of the algorithm, the next few examples demonstrate how the other traditional limitation of IP has been overcome, specifically that of the invasion front always occurring via a single point. Figure 14 shows the same geometric model configuration having a three-point invasion scheme. The source points are located in three successive layers and ''feed'' petroleum into the system at a constant and equal rate.

Early in the invasion process (Figure 14a), each invasion cluster expands independently. Later (Figure 14b), the clusters coalesce, and the aggregate charging volumes of the new, unified cluster are equal to the input from the joined source systems. In Figure 14c, the upper cluster is now flowing out of the open vertical boundary, whereas the lowest cluster expands beneath the lowest baffle. In Figure 14d, the lowest baffle is breached, and the two remaining clusters coalesce.

For real petroleum systems, the assumption of a constant feed rate would not properly represent what occurs in the creation of a secondary petroleum migration system. For example, expulsion rates and

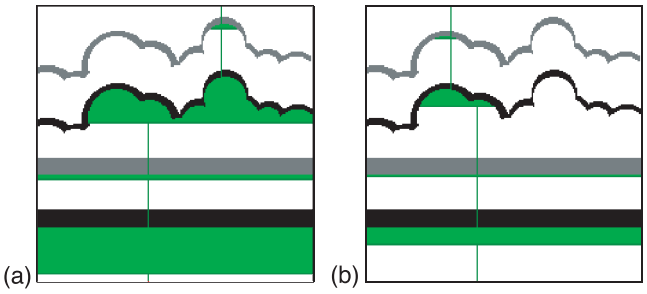

Figure 13. Effect of changing the density contrast (and holding the threshold pressures constant). The grid cell size is set to 1 m in all directions: (a) density contrast of 300 kg/m^3, (b) density contrast of 800 kg/m^3.

volumes will be a function of total organic content, temperature, maturity, source rock thickness, etc., all of which will vary as a function of location and of time.

Figure 15 shows the results of using the same configuration as depicted in Figure 14, where the input rates are unique for each source point. Although in this example the source rates are constant (but different) for each source point, there is no reason to keep the rates constant. Indeed, we have created many simulations where the source rates for multiple (e.g., 200,000+) source points varied as a function of location and time (e.g., Zwach and Carruthers, personal communication, 1998; Figure 16).

Models having these simple configurations are extremely valuable in validating the mechanisms assumed by the algorithm, but to be of significant value, the complexity of the geometries must better represent geologic systems. Because the transport routines are so efficient, simulations can be carried out on multimillion grid cell models in a matter of minutes, thereby providing virtually limitless applications for solving the transport problem through realistic fabrics.

Consider the example depicted in Figure 17. This case simulates the horizontal migration of oil through a core-scale section of highly bioturbated deposits. The model contains 5.4 million grid cells, and the threshold pressures were set based on estimates of the clay content of each cell (the higher the clay content, the higher the threshold pressure, broadly equal to the gray scales depicted in the images). The left boundary was set to a ''closed'' state; all others were open. As with some of the earlier examples, the colors represent invasion times of the grid cells.

This particular simulation was executed in well under 1 min and highlights the importance of the fabric itself in defining migration trajectories and saturations. Subtle variations in threshold pressures can effectively shield entire regions from seeing the oil (e.g., the lower quarter of the model). It is also true that it is the configuration of the baffles and seals that has the greatest impact on trajectories. In this case, the oil follows the paths defined by the boundaries of the highest threshold pressure (darkest) sediments.

This type of simulation can be used to perform capillary equilibrium upscaling. For example, once this volume is spanned horizontally, the critical saturation (i.e., the first nonzero oil relative permeability) and the horizontal threshold pressure can be calculated. Additionally, a separate vertical invasion scheme would provide critical parameters for an upward invasion. Combined, these give the anisotropic, critical parameters for this particular volume and lithotype, which could then be used as input into reservoir or basin simulators.

Figure 18 shows the tool applied to an outcrop-scale example. Here, an interpreted outcrop (shallow marine) panel was converted to a capillary threshold pressure lattice, based on permeability–threshold pressure relationships. The model assumed that oil

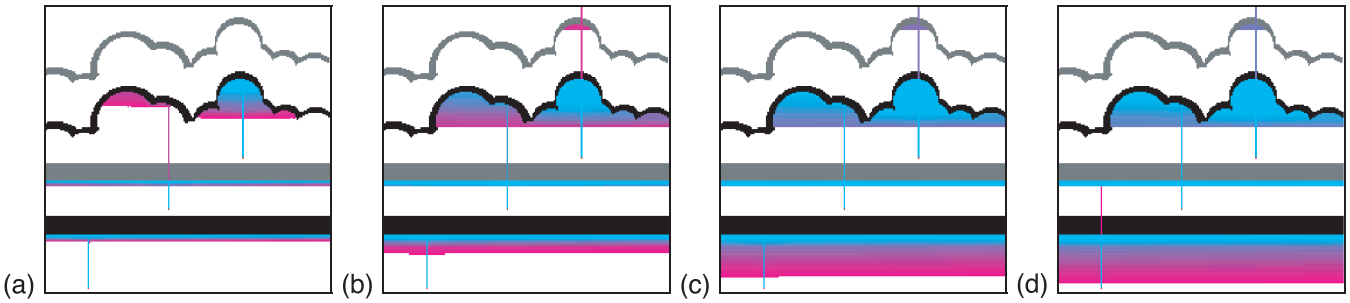

Figure 14. Saturation profiles for a multipoint invasion scheme (three source points). The vertical boundaries are open; the horizontal boundaries are closed. Colors represent invasion times (blue early, magenta late). A density contrast of 300 kg/m^3 and a vertical grid cell size of 1 m were used.

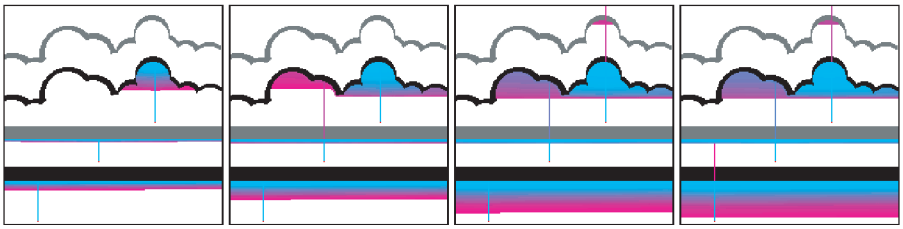

Figure 15. Saturation profiles for a multipoint, variable-charge rate invasion scheme. The vertical boundaries are open; the horizontal boundaries are closed. Colors represent invasion times (blue early, magenta late). The lowest invasion point is expelling oil at a fast rate, the midpoint at a slow rate, and the upper point at a medium rate.

entered from the east and invasion continued so long as the expansion of the cluster occurred in the open boundaries.

As with the previous core-scale example, it is the fabric of the nonreservoir units (in this case the shales) that controls migration trajectories.

This type of simulation is well suited for estimating loss rates and migration efficiencies through various carrier types. Although an accumulation is clearly seen, it may be too small to be of any economic significance; therefore, any oil saturations along this carrier section would be considered a loss, thereby reducing the migration efficiency (where migration efficiency is expressed as the fraction of petroleum that leaves point A and arrives at point B).

These past two examples were 2-D, but the algorithm works just as well in three dimensions. The only difference is an increase in the coordination number. In fact, the speed of the algorithm is a function of the number of invaded sites, and as discussed in the section on IP modeling, the percolation threshold is lower in three dimensions than it is for two dimensions. For a 2-D and 3-D system having the same number of grid cells, the invasion algorithm works faster on the 3-D case. An interesting consequence of the differences between 2-D and 3-D percolation thresholds is that the saturation volumes will be different between the two cases (higher in 2-D than in 3-D). This suggests that volumetric calculations based on 2-D models are likely to be grossly inaccurate.

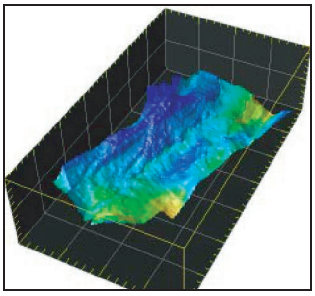

Figure 16. Expulsion map created using QuickVol3D (Zwach et al., 2000). Using schemes such as this, the spatial configuration of the source points (or areas) can be defined, along with rates and compositions, for basin-scale simulations.

Figure 19 shows the results of a 3-D basin-scale simulation. The model contains 15 million grid cells and executed in less than 5 min on an SGI equipped with an MIPS R1000 CPU. Thousands of concurrent source points were specified using a scheme similar to that depicted in Figure 16. Shown in Figure 19 are the saturation profiles represented in terms of actual saturations (Figure 19a) and invasion times (Figure 19b). Also shown is a key formation surface for spatial reference.

The model was built by stacking formation surfaces and in-filling the 3-D volume. Fault surfaces were then inserted into the volume (Figure 20), and each flow unit (including the faults) was assigned threshold pressures, in this case based on porosity and permeability estimates.

Because the model scales correctly (i.e., the correct relationship between column heights and capillary threshold pressures is maintained at all length scales), the input threshold pressures of the various formations were derived from calibrations to known column heights. In other words, because the column height beneath a seal is known, this must define the minimum threshold pressure of the seal, and this information can be used to populate the model with realistic parameters.

These types of high-resolution 3-D models enable the calculation of detailed volumetrics. As with the outcrop model, migration efficiencies can be calculated in addition to the direct determination of emplaced petroleum volumes in each accumulation.

Fifteen million grid cells is already orders of magnitude higher than the resolution limits of full Darcy-based transport solvers, but even larger models are possible. The only limitation to the model's resolution is one of computer memory, with each grid cell currently using approximately 50 bytes of memory. With the price of memory being very low, we have for this first time the possibility of performing secondary migration transport modeling on seismic

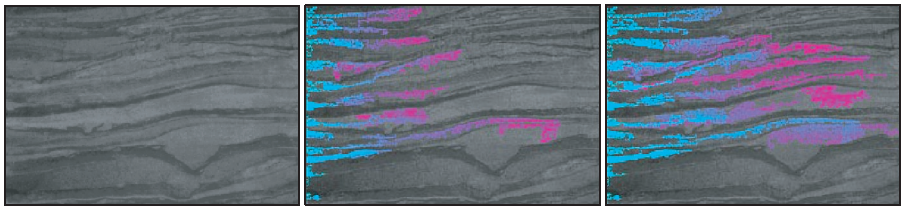

Figure 17. Simulating horizontal migration through a bioturbated volume. The model consists of 5.4 million grid cells with each grid cell having a length scale of 0.1 cm. Density contrast was set to 300 kg/m^3.

resolution (average cell size down to 15–30 m) volumes, which would enable for the first time calibration of petroleum system modeling to seismic scale, direct hydrocarbon indicators.

DISCUSSION AND FUTURE WORK

The new modeling techniques presented in this chapter offer the potential to conduct transport simulation at unprecedented resolutions. However, as mentioned in the introduction, the transport problem is only one aspect of the larger secondary petroleum migration modeling problem. To truly address this larger subject area, these modeling algorithms need to be extended to include a broad range of variables that affect petroleum systems through geologic time.

Fortunately, these algorithms are extensible, and as a first step, the inclusion of additional petroleum system variables can be handled through linkages with external basin modeling packages. It is suggested that these transport algorithms could be included as an alternative transport scheme in basin modeling packages. Rather than relying on the full (and slow) Darcy-based solvers, these new techniques could be used as a replacement, thereby freeing up an enormous amount of CPU cycles that could be redirected to increasing the resolution of basin models. In this way, dynamic phase properties and dynamic basin geometries could be coupled with this new transport scheme.

It should be possible to do compositional modeling with these types of tools, because so many of the transport variables that are important for compositional modeling are captured during the simulation process. These variables include phase properties at the source, a detailed history of where the fluids have been, the paths they have taken, the transport times involved, which rock volumes they have passed through, and the residence time of the fluids in the pathways and accumulations. However, the current algorithm is limited to the simulation of a fluid having a single component, operating under constant pressure-volume-temperature (PVT) conditions.

These constant conditions are clearly unrealistic for a petroleum migration scenario, but the algorithms could be extended to include the effects of fluid compositions by tracking the characteristics of the (multicomponent) clusters as they move through PVT space. Clusters would no longer be limited to a binary state of presence but could include detailed phase and composition information that would change through time. In theory, phase calculations and the determination of density and interfacial tension could be handled via lookup tables to keep run times to a minimum.

Another use for these types of tools is in the area of pathway and prospect risking. At the exploration stage, huge uncertainties exist in the parameterization of these models. Therefore, the ability to quickly evaluate multiple realizations covering the range of uncertainties is of obvious value. We have already implemented such a scheme whereby the threshold pressures, porosities, and saturation function end points are all expressed in terms of probability density functions (PDF). Multiple realizations can be created that sample these PDF, and

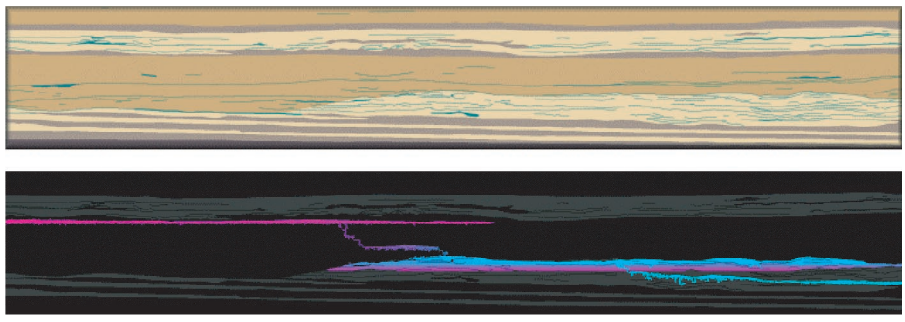

Figure 18. Migration through an outcrop-scale (1 km × 20 m) section of a shallow marine sequence. Petroleum originates from a lower carrier to the east of the figure. The model contains almost 3 million grid cells. The upper image depicts the interpreted outcrop photo panel, while the lower depicts the invasion profile, colored by invasion time (the background panel is shown in dark colors to increase visual clarity).

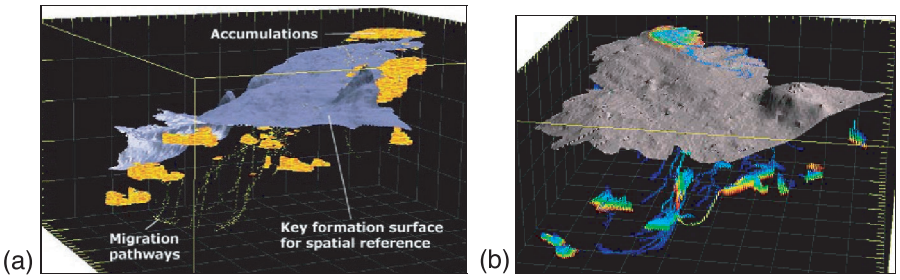

Figure 19. 3-D basin-scale results of the new transport routines. The model contained 15 million grid cells and executed in less than 5 min on a modest workstation. Depicted are the low-oil-saturation migration pathways and the high-saturation accumulations.

the output of these realizations can be compared and ranked according to a final set of ''known'' conditions. For example, one could create *n* realizations and indicate that only those realizations that honor the location of known accumulations should be accepted. If those realizations honor these known locations and they estimate the location of unknown reserves, then this greatly increases the confidence one would associate with these new reserves (perhaps some of the new genetic algorithms coming from the computer science disciplines could be used for this type of risking).

Although these models have obvious benefits for basin-scale modeling, the techniques can be applied to improve our understanding of reservoirs as well. Typically, very detailed, multimillion grid cell models of reservoirs are created, only to be ''upscaled'' for flow modeling to the point where many geologic features are no longer distinguishable. These new migration tools could be used to charge the high-resolution reservoir models with petroleum, leading to an increased understanding of petroleum emplacement patterns in different reservoir architectures, without the need for any upscaling. Once it is determined where the petroleum is emplaced, well placement and varying completion strategies could be evaluated to maximize recovery.

The number of potential applications is vast, because for the first time, significant computation times may no longer be an obstacle to simulation.

CONCLUSIONS

Petroleum migration occurs in a state of capillary equilibrium in a flow regime dominated by gravity and capillary forces. In this regime, viscous forces are insignificant with the consequence that variables critical for solving the transport problem at reservoir production timescales become irrelevant for migration timescale flows.

For migration to occur through a given rock volume, a critical saturation is required to form a spanning cluster across the rock volume. This saturation corresponds with the saturation of the first nonzero petroleum-relative permeability and defines the precise instance when flow will occur. The pressure in the petroleum phase at this critical saturation is termed the threshold pressure, and this pressure is one of the only variables needed to solve the transport problem.

Where the petroleum saturations are at the critical saturation, it is very likely that the petroleum will be snapped off (discontinuous), meaning that these areas are not contributing to the development of any pressure heads needed to breach any upstream baffles. Where accumulations (at any length scale) form, saturations will approach the connate water saturation, and connectivity in the petroleum column will contribute to a pressure head.

Invasion percolation modeling has historically been used to simulate the transport of a nonwetting phase through a wetting phase–saturated environment. These models assume capillary equilibrium conditions and have accurately reproduced results derived from small-scale invasion experiments. These models have assumed ubiquitous continuity in the invading phase, thereby limiting their scale of applicability to samples generally less than a meter in size.

New techniques have been developed that remove the scaling limitations of IP modeling while honoring the mechanics of migration transport processes. These new techniques have been shown to properly honor the force balance and fluid equilibrium

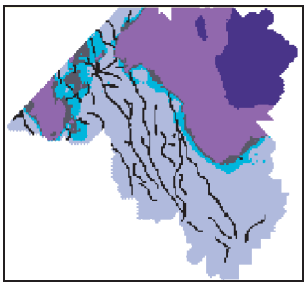

Figure 20. Horizontal slice through the model depicted in Figure 19 showing the arrangement of various flow units, including faults, for one layer.

conditions for models ranging from the core scale to the basin scale.

These new techniques also enable the simulation of multiple charge points or areas, operating concurrently. The rates associated with these charge points can vary through time, allowing for the use of geologically realistic expulsion and carrier feeding schemes.

These new techniques are extremely computationally efficient, with transport models containing tens of millions of grid cells being solved in a matter of minutes. For the first time, it may be possible to create transport simulations on basin-scale models having seismic property resolutions. In addition, the speed of the technique leaves ample processing room for the inclusion of additional calculations that could collectively be used to offer greater insights and predictive modeling capabilities to petroleum systems analysis.

ACKNOWLEDGMENTS

I would like to acknowledge and thank the following companies for their continued support of this research: ENI Agip Division, BG Technology, BP, Conoco, Norsk Hydro, Shell, and Statoil.

I would also like to thank Norsk Hydro and BG Technology for permission to publish Figure 16 and Figure 19, respectively, and the Genetic Units Project at Heriot-Watt University for use of their outcrop data in creating the model depicted in Figure 18.

I would also like to acknowledge the valuable input of my colleague, Mike de Lind van Wijngaarden, for making these modeling tools as fast (and as accurate) as they are.

REFERENCES CITED

Berg, R. R., 1975, Capillary pressures in stratigraphic traps: AAPG Bulletin, v. 59, p. 939–956.

Broadbent, S. R., and J. M. Hammersley, 1957, Percolation processes, I: Crystals and mazes: Proceedings of the Cambridge Philosophical Society, v. 53, p. 629–641.

Carruthers, D. J., 1998, Transport modeling of secondary oil migration using gradient-driven, invasion percolation techniques: Ph.D. dissertation, Heriot-Watt University, Edinburgh, U.K., 210 p.

Carruthers, D., and P. Ringrose, 1998, Secondary oil migration: Oil-rock contact volumes, flow behaviour and rates, *in* J. Parnell, ed., Dating and duration of fluid flow and fluid-rock interaction: Geological Society (London) Special Publication 144, p. 205–220.

Catalan, L., F. Xiaowen, I. Chatzis, and F. A. Dullien, 1992, An experimental study of secondary oil migration: AAPG Bulletin, v. 76, p. 638–650.

Chandler, R., J. Koplik, K. Lerman, and J. F. Willemsen, 1982, Capillary displacement and percolation in porous media: Journal of Fluid Mechanics, v. 119, p. 249–267.

Chatzis, I., and F. A. Dullien, 1983, Dynamic immiscible displacement mechanisms in pore doublets: Theory vs. experiments: Journal of Colloids and Interface Science, v. 91, no. 1, p. 199–222.

Dembicki, H., Jr., and M. J. Anderson, 1989, Secondary migration of oil: Experiments supporting efficient movement of separate, buoyant oil phase along limited conduits: AAPG Bulletin, v. 73, no. 8, p. 1018–1021.

England, W. A., A. S. Mackenzie, D. M. Mann, and T. M. Quigley, 1987, The movement and entrapment of petroleum fluids in the subsurface: Journal of the Geological Society of London, v. 144, p. 327–347.

Frette, V., J. Feder, T. Jossang, and P. Meakin, 1992, Buoyancy-driven fluid migration in porous media: Physical Review Letters, v. 68, p. 3164–3167.

Furuberg, L., J. Feder, A. Aharony, and T. Jossang, 1988, Dynamics of invasion percolation: Physical Review Letters, v. 61, p. 2117–2120.

Haines, W. B., 1930, Studies in physical properties of soils, V: The hysteresis effect in capillary properties and the modes of moisture distribution associated therewith: Journal of Agricultural Science, v. 20, p. 97.

Hirsch, L. M., and A. H. Thompson, 1995, Minimum saturations and buoyancy in secondary migration: AAPG Bulletin, v. 79, p. 696–710.

Meakin, P., J. Feder, V. Frette, and T. Jossang, 1992, Invasion percolation in a destabilising gradient: Physical Review A, v. 46, p. 3357–3368.

Meakin, P., G. Wagner, V. Frette, T. Jossang, J. Feder, and A. Birovljev, 1994, Gradient-driven migration in porous media: Experiments and simulations: North Sea oil and gas reservoirs III: Norwegian Institute of Technology (NTH), p. 297–305.

Rasmussen, B., 1997, Fluorescent growth bands in irradiated-bitumen nodules: Evidence of episodic hydrocarbon migration: AAPG Bulletin, v. 81, no. 1, p. 17–25.

Schowalter, T. T., 1979, Mechanics of secondary hydrocarbon migration and entrapment: AAPB Bulletin, v. 63, p. 723–760.

Thomas, M. M., and J. A. Clouse, 1995, Scaled physical model of secondary oil migration: AAPG Bulletin, v. 79, p. 19–29.

Wilkinson, D., 1984, Percolation model of immiscible displacement in the presence of buoyancy forces: Physical Review A, v. 30, p. 520–531.

Wilkinson, D., and J. Willemsen, 1983, Invasion percolation: A new form of percolation theory: Physics Abstracts, v. 16, p. 3365–3376.

Zwach, C., T. Throndsen, and J. Bergan, 2000, Quick mapping of basin modelling results — A key for quantifying prospect sensitivities, *in* K. Ofstad, J. E. Kittilsen, and P. Alexander-Marrack, eds., Amsterdam, Elsevier: Norwegian Petroleum Society (NPF) Special Publication No. 9, p. 159–170.